Macroendocytosis and endosome processing in snake motor boutons

Haibing Teng, Michael Y. Lin and Robert S. Wilkinson

Department of Cell Biology and Physiology, Washington University School of Medicine, St Louis, MO, USA

We have examined the processing of endosomes formed by macroendocytosis (ME), or bulk membrane retrieval, in active motor terminal boutons at the snake nerve–muscle synapse. Endocytic probes were imaged at light (FM1–43) and electron (horseradish peroxidase (HRP)) levels over stimulus frequencies representing low, intermediate and high levels of use. Endosomes formed rapidly (1–2 s) at all frequencies, concomitant with clathrin-mediated vesicular endocytosis (CME). Endosomes dissipated rapidly into vesicles (∼10 s). The dissipation rate was not influenced by activity. Many endosomes split into clusters of 2–20 smaller endosomes of varying size. Vesicles budded from these smaller endosomes, from large endosomes that had not undergone fission into smaller ones, and from precursor membrane infoldings that had not yet internalized. In snake, exocytosed vesicular membrane is not competent for reuse until after a delay (> 3 min). We found that time required for endosome processing is not responsible for this delay. Endosome processing might, however, limit availability of some vesicles for release at very high levels of use. Generally, endosome processing paralleled that of vesicles internalized directly from the plasma membrane via CME, regardless of stimulus frequency. There was no evidence for differential recruitment of ME *versus* CME depending upon level of use.

(Received 26 February 2007; accepted after revision 1 May 2007; first published online 3 May 2007)
Corresponding author R. S. Wilkinson: Department of Cell Biology and Physiology, Washington University School of Medicine, 660 South Euclid Av., Box 8228, St Louis, MO 63110, USA. Email: wilk@wustl.edu

Macropinocytosis, or bulk membrane infolding and retrieval, is a long-known mechanism by which cells 'drink' samples of their extracellular milieu to create large (> 100 nm) irregularly shaped endosomes (reviewed by Conner & Schmid, 2003). More recently, a similar mechanism has been associated with compensatory endocytosis in nerve terminals. Here the purpose is not internalization, but retrieval of spent vesicular membranes and vesicular membrane proteins following transmitter release (Miller & Heuser, 1984; but see also Holt *et al.* 2003). The process, which we refer to as macroendocytosis (ME; the formation of endosomes substantially larger than transmitter-containing vesicles), has been observed in many types of nerve terminals (reviewed by Royle & Lagnado, 2003; most 'cisternae' seen in EM sections are probably the result of ME). A current two-component vesicle processing model consists of ME (the first component) plus a different type of endocytosis that takes place near active zones (AZs). This second, local component of endocytosis is either 'kiss-and-run' transmitter release or clathrin-mediated endocytosis (CME) directly from the plasma membrane (see LoGiudice & Matthews, 2006). The model's key feature is that local endocytosis and ME serve distinct functions. Local endocytosis is the entry point of a local recycling pathway that reforms vesicles for rapid reuse at a particular AZ (rapid recycling). In contrast, ME recycles vesicles into a large (reserve) pool from which they are mobilized for reuse more slowly. ME is associated with high levels of neural activity (high stimulus frequencies) while local endocytosis is associated with low activity levels (low stimulus frequencies; Gad *et al.* 1998; Richards *et al.* 2000). Kinetically, ME is thought to be slow (minutes) compared with local endocytosis (seconds), based on the time course of capacitance measurements as well as optical studies (Richards *et al.* 2000; de Lange *et al.* 2003; Royle & Lagnado, 2003). Thus, rapid exocytosis at high stimulus frequencies recruits, paradoxically, slow compensatory endocytosis, and *vice versa* Evidence supporting this two-component model has come from the frog neuromuscular junction (NMJ) Richards *et al.* 2000, 2003), *Drosophila* NMJ (Koenig & Ikeda, 1996; Kuromi & Kidokoro, 1998), the mammalian calyx of Held (Sun *et al.* 2002; de Lange *et al.* 2003), goldfish retinal bipolar terminals (Neves *et al.* 2001), lamprey reticulospinal terminals (Gad *et al.* 1998) and other preparations. An exception is rodent hippocampal terminals, which, perhaps because of their small size,

This paper has online supplemental material.

 DOI: 10.1113/jphysiol.2007.130989

lack ME; these can rapidly recycle synaptic vesicles at all stimulus frequencies (Pyle *et al.* 2000; Ertunc *et al.* 2007).

The same two components of endocytosis (ME plus CME) comprise an alternative vesicle processing model as well. We have observed ME, as well as CME near active zones, in motor terminals of snake (Teng *et al.* 1999; Teng & Wilkinson, 2000). In the model above, these two endocytic modes serve as entry points for a pair of distinct vesicle processing pathways. However, snake motor terminals lack local recycling, and instead utilize the reserve vesicle pool at both low and high levels of activity (Lin *et al.* 2005). This disparity raises a question as to the nature of ME in snake terminals. Are ME and CME recruited differentially, as has been reported in other species, yet complement each other so that no apparent change in recycling strategy with frequency is seen? Alternatively, do ME and CME occur at all frequencies, and in the same proportion, so that both contribute to reserve pool cycling in a frequency-independent manner? To answer this question we have examined ME in snake motor terminals stimulated at three frequencies representing low, moderate and high physiological levels of use — 0.3 Hz, 3 Hz and 30 Hz. ME contributed to vesicle processing approximately equally at all frequencies. ME was rapidly initiated, and it was universally employed, including at very low levels of use. Endosomes were rapidly internalized (1–2 s) and rapidly dissipated (∼10 s). Indeed, we found the dynamics of ME during the first minute after stimulation to be quite similar to those of CME. Dissipation was via vesicle budding but also via fission into smaller endosomes, a process not previously described. The occurrence of ME at all levels of use suggests an important functional role that extends beyond that of supplementary membrane retrieval at high stimulus rates.

Methods

Garter snakes (*Thamnophis sirtalis*) were anaesthetized with pentobarbital sodium (80 mg kg^{-1}, I.P.) and immediately killed by rapid decapitation. Several contiguous segments of the single-fibre-thick trans-versus abdominis muscle were dissected from the animal, placed in reptilian saline solution (composition in millimolar concentration NaCl, 145; KCl, 2.5; $CaCl_2$, 3.6; $MgSO_4$, 1.8; KH_2PO_4, 1.0 HEPES, 5.0; NaOH as needed for pH 7.4) and divided to provide 3–10 individual nerve–muscle preparations. Each preparation contained three small segmental muscles (∼50 singly innervated twitch fibres, plus tonic fibres, which were not studied). Nerve terminals innervating twitch fibres comprise ∼58 discrete boutons, similar to boutons in the mammalian nervous system. All procedures followed the Washington University Guidelines for Animal Studies. All experiments were performed at room temperature (25°C).

Electrical stimulation and activity-dependent staining

Preparations were pinned into a dish containing reptilian saline solution. The centre muscle's nerve was placed within a suction electrode connected to an isolated stimulator. The two adjacent muscles served as unstimulated controls. A single stimulus was delivered to confirm that the muscle twitched; the preparation was then rested for > 5 min. During experiments, pre-programmed stimulus trains (200 μs rectangular pulses adjusted to be superthreshold, ∼7 V) were delivered as described in Results.

During stimulation, the bath contained either dye-free saline solution, or saline solution plus dye. Activity-dependent dyes were FM1-43FX (varying concentration, see below; Invitrogen, Carisbad, CA, USA), FM4-64 (13 μm; Invitrogen), tetramethylrhodamine-dextran (10 kDa or 70 kDa; 50 μM; Invitrogen), or HRP (10 mg ml^{-1}, Sigma, St Louis, MO, USA). The lectin fluorescein-VVA (67 μg ml^{-1}; Vector laboratories, Inc., Burlingame, CA, USA) was added to label the synaptic cleft (details in Teng *et al.* 1999) in dextran experiments. VVA was in the bath for 30 min and then washed out (saline, ×3, 10 min each) before stimulation. Concentration of FM1-43FX was 2 μM except in the 30 Hz continuous stimulation experiments of Fig. 6 (2 μM for time points of 3, 9, 18, 36 s; 1 μM for 60 s; 0.5 μM for 120 s; 0.25 μM for 240 s) and Fig. 7 (1–1.5 μM for time points of 18 s; 1 μM for 60 s; 0.5 μM for 120 s; 0.25 μM for 240 s).

FM1–43 or dextran was dissolved in reptilian saline and applied to the bath before the period of electrical stimulation. Both dyes were easily washed out in 10–20 s before fixation (saline, ×3–6, ∼3 s each). Fixation was with 4% formaldehyde in 100 mM sodium phosphate buffer, 30 min at room temperature, followed by a 30 min wash in PBS.

Light microscopy

We imaged fixed tissue with a 63×, 1.4 NA oil immersion lens to provide high resolution and to avoid possible light damage (slowing of endosome dissipation seen in preliminary experiments) associated with use of living tissue. Use of fixed tissue also allowed us to prepare specimens for EM using protocols identical to those used at light level. We used a different nerve–muscle preparation from the same snake for each time point. To do so we took advantage of the snake's unique anatomy, from which dozens of nearly identical segmental muscles can be obtained from one animal. A Zeiss LSM-510 confocal microscope with META adaptor was used. Nerve terminals were imaged in 7–44 planes, separated by *z*-axis steps of 370 nm. Details of tissue preparation and imaging are provided elsewhere (Teng *et al.* 1999). Epifluorescence images using two different coloured dyes

were obtained using META to reduce bleed-through, after first calibrating the META photometer with each dye.

Measurement of endocytosed structures

We used region-of-interest software (Scion Image, Scioncorp.com) to manually outline boutons and individual endosomes within bouton. All remaining measurements were automated. Size (area) and average brightness of each endosome was calculated, as was average brightness of entire boutons, plus average brightness of vesicle 'haze' within boutons (bouton brightness minus the contribution of endosomes). Brightness is expressed as arbitrary pixel brightness units, ABUs, in the range from 0 to 255. Microscope adjustments, and thus actual fluorescent dye uptake per ABU, were held constant during all measurements for experiments of Figs 1–5 and 8 and 9. To observe ensosomes with longer stimulation (Figs 6 and 7), settings (laser power, gains, offset) were adjusted optimally for each time point. Reduced data from averaged measurements included average endosome size, number of endosomes, total bouton area occupied by endosomes, and average endosome brightness. Measurement of endosome size seemed most prone to scatter.

Electron microscopy

We chose HRP, rather than photoconversion of FM1-43, because HRP provided a larger sample size – virtually every nerve terminal in the muscle. Preparations were rested 1–2 h after dissection before beginning experiments. HRP (10 mg ml^{-1}) was applied to the bath 5 min before stimulation. Care was taken to ensure that HRP did not irritate the muscle nerve – twitches of the muscle were watched throughout the loading process. Details, including use of a reaction product of HRP as an electron-dense marker, were as previously described (Teng & Wilkinson, 2000) except that no counterstaining was used. EM negatives were scanned into a computer and displayed for analysis using methods described elsewhere (Teng & Wilkinson, 2000).

Results

We asked how and when endosomes form, how long they remain patent to the extracellular space (synaptic cleft) and how they dissipate into vesicles. Observations were with confocal light microscopy (which provided a large sample size) and transmission EM (which provided high resolution), both using fixed tissue. To visualize endosomes with light we used FM1-43 and fluorescein-dextran as fluorescent endocytic probes. To visualize endosomes with EM, we used HRP as a fluid-phase marker.

Properties of endosomes viewed at light level

At light level, putative endosomes remained visible throughout most of their life as bright discrete structures. To confirm that these structures were indeed formed by ME and not vesicle fusion we compared staining of boutons loaded with 10 kDa rhodamine–dextran, which enters both endosomes and vesicles, to staining of boutons loaded with 70 kDa rhodamine–dextran, which can enter large endosomes but not vesicles (Berthiaume *et al.* 1995; Holt *et al.* 2003). The small dextran revealed endosomes as punctate structures, and endocytosed vesicles as a diffuse haze (Fig. 1*A*, red; the synaptic cleft is

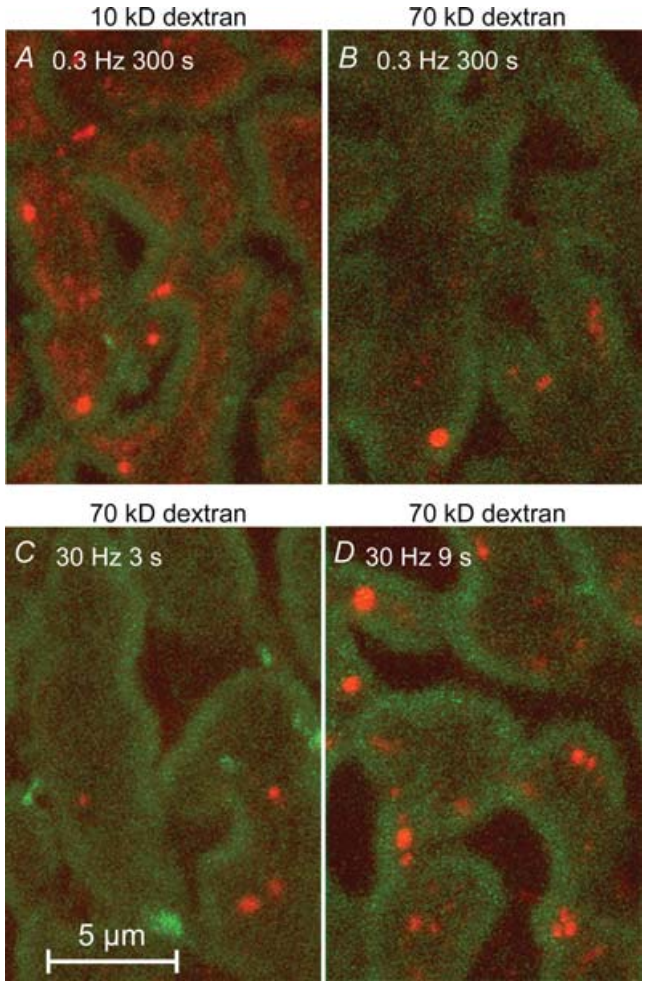

Figure 1. High MW dextran (70 kDa) enters endosomes formed via ME but does not enter vesicles
Shown are a few boutons from one terminal in each of 4 preparations; synaptic clefts outlining the boutons are stained with the lectin fluorescein-VVA (green). *A*, control terminal loaded with low MW rhodamine–dextran (10 kDa, red) by 0.3 Hz, 300 s stimulus train. Both endosomes (bright punctate structures) and vesicles (haze) took up the dye, similar to uptake of FM1-43. *B*, terminal loaded by the same stimulus train, but with 70 kDa rhodamine–dextran (red) showed uptake by endosomes but not most vesicles. *C* and *D*, results were similar with 30 Hz stimulation. The number of structures stained increased with stimulus duration.

labelled with fluorescein VVA, shown green). In contrast, the large dextran showed only the punctate structures, indicating that these structures had been internalized via a larger opening than that of a vesicle, and were therefore macroendosomes (Fig. 1*B*; protocol identical to that of Fig. 1*A*). The large dextran was taken up at both 0.3 Hz and 30 Hz stimulus frequencies; the number of stained structures increased with increasing stimulus duration (Fig. 1*B–D*).

Frequency dependence of endosome formation

We compared endosomes formed in response to 90 stimuli delivered at each of three frequencies: 0.3, 3 and 30 Hz. Preparations were washed (10 s) beginning immediately after the stimulus period and then fixed. Due to frequency-dependent synaptic depression, total transmitter release was greatest at 0.3 Hz, slightly reduced at 3 Hz, and substantially reduced (by ∼70%) at 30 Hz (Lin *et al.* 2005). Compensatory endocytosis in direct proportion to release (see Lin *et al.* 2005), is evident from the overall staining intensity of the three example terminals in Fig. 2*A* and from the bar graph of Fig. 2*B* (data from 626 to 731 boutons in 17–22 NMJs from 3 snakes). Characteristics of the endosomes that contributed to the overall staining of boutons are in Fig. 2*C–E*. Endosomes were of similar average size (∼0.2 μm^2) at both lower frequencies, but were significantly smaller with 30 Hz stimulation (∼0.1 μm^2; $P < 0.01$). Conversely, the number of endosomes per bouton was similar (∼1) at the two lower frequencies but significantly greater (∼2; $P < 0.01$) at 30 Hz (Fig. 2*D*). Thus the total fraction of a typical bouton's surface area that was occupied by endosomes was similar at all frequencies (1.8 ± 0.2%; Fig. 2*E*). However, because overall staining (endosomes plus vesicles) decreased with frequency (Fig. 2*A* and *B*), the fraction of internalized dye contained in endosomes rather than vesicles was actually greater after brief high frequency stimulation (Fig. 2*A*; compare upper and lower panels), presumably because time was not allowed for complete dissipation of endosomes into vesicles prior to fixation (see below). Consistent with this, endosomes that formed at various times during a 5 min period before fixation (0.3 Hz; Fig. 2*A*) were of disparate shapes – some being large, 'fuzzy' and irregular, consistent with partial dissipation into clusters of vesicles or smaller endosomes (arrowhead; see EM results below), with others being smaller and punctate (arrow). When shorter times were allowed (3 Hz, 30 Hz; Fig. 2*A*) endosome shapes were more consistently punctate.

Time course of endosome formation and dissipation

To estimate the time required for endosome formation we employed two different-coloured dyes. Three protocols were used with each of three stimulation trains (90 stimuli at 0.3, 3 or 30 Hz; Fig. 3). In the first protocol, FM1-43 (green) was present during stimulation, then (with the preparation resting) rapidly exchanged with FM4 64 (red), which remained for 60 s before washing (20 s) and fixation. In the second protocol, the dye change was delayed for 10 s after completion of stimulation, while in the third, the dye change was delayed for 60 s. Images of a few boutons from terminals stained according to the first protocol are in Fig. 3*A*. At 0.3 Hz frequency there was no red signal in any protocol, indicating that virtually all endocytosis was completed during the stimulation (100%; Fig. 3*B*; 7 NMJs at each delay time, 1 snake). As expected, we saw few endosomes at this frequency (example, green arrow), presumably because most of them had already dissipated into vesicles (bright haze) during the 300 s stimulation period. In contrast, 3 Hz, 30 s and 30 Hz, 3 s protocols revealed endosomes internalized both before (green structures) and after (red structures, red arrows) the stimulation was complete. Some endosomes began forming during exposure to FM1–43 and remained patent to the cleft during subsequent exposure to FM4-64 as well, and therefore contained both dyes (yellow structures, yellow arrows). Results are summarized in Fig. 3*C* (3 Hz, 30 s; $n = 308–647$ boutons, 12–24 NMJs at each delay time, 3 snakes) and Fig. 3*D* (30 Hz, 3 s; $n = 155–203$ boutons, 7 NMJs at each delay time, 2 snakes). The total number of endosomes seen decreased substantially with time after stimulation (not shown; see Figs 4 and 5) but that number is shown normalized to 100% at each time point. Of those endosomes, a significant fraction were formed up to 60 s after stimulation (Fig. 3*C* and *D*). The number of endosomes that contained both dyes was substantial (4% to 14%), indicating that endosomes remained patent to the bath for some time (see Discussion).

The short duration of our standard 30 Hz protocol provided in effect a 'pulse' of exocytosis. This allowed us to examine in detail the subsequent time course of endocytosis using FM1–43 (Figs 4 and 5). To do this we first measured the average dye uptake rate (brightness/time in dye) during the 3 s stimulation and during 15 s periods of dye application beginning at various times after the end of stimulation (0, 15, 30 or 60 s). Preparations were washed (15 s) and fixed before imaging. Results ($n = 315–357$ boutons, 9–10 NMJs per data point, 2 snakes) are in Fig. 4. The endocytic rate fell monotonically with time after stimulation and was near zero after ∼20 s. We measured total average bouton brightness due to endosomes (ME, right scale) and vesicle haze (CME, left scale) separately. The two processes operated in parallel, decaying with nearly identical time courses (single exponential fits: haze, 3.45 s; endosomes, 3.8 s; Fig. 4*A*). The size of endosomes was about the same whether they were formed during stimulation or afterward (Fig. 4*B*). The number of endosomes formed per second decreased with roughly the same

time course as their overall brightness (Fig. 4*C*, compare with Fig. 4*A*). Together with the observation of constant size, this indicates that the brightness (dye content) of an endosome was on average the same whether formed during or after stimulation.

We next measured the overall dye uptake when FM1–43 was applied to the bath during 30 Hz, 3 s stimulation and allowed to remain for various times after stimulation before rinsing (20 s) and fixation (Fig. 5; $n = 223$–297 boutons per data point, 9–10 NMJs, 2 snakes). Uptake (vesicles plus endosomes) increased substantially during the 15 s immediately following stimulation, then increased slowly or levelled off thereafter (Fig. 5*A*). Endosome size (mean area) increased slightly, then slightly decreased; neither change was significant (Fig. 5*B*). In contrast, the number of endosomes (Fig. 5*C*) and the fraction of

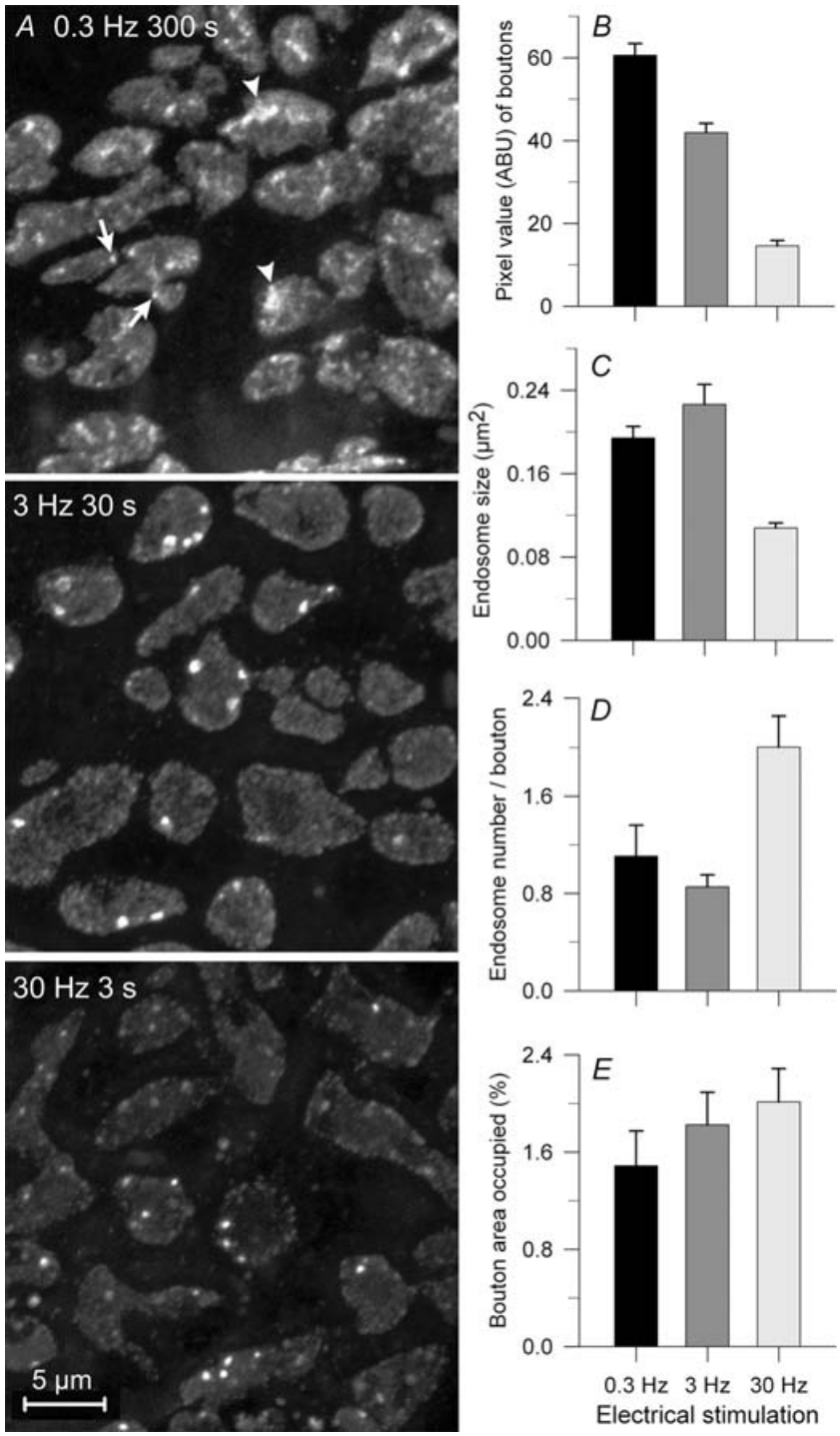

Figure 2. Formation of endosomes by 90 stimuli delivered at different frequencies
A, a few boutons from terminals activated at low, medium and high frequency in FM1-43 bath. Overall staining was brightest at 0.3 Hz (note haze from vesicular dye uptake). Endosomes at 0.3 Hz were either punctate (arrows) or fuzzy (arrowheads). Endosomes at 30 Hz were mostly punctate and more numerous than those at lower frequencies. *B*, overall dye uptake decreased with increasing frequency due to frequency-dependent depression (see text). *C*, endosomes were smaller at 30 Hz than at lower frequencies. *D*, the number of endosomes per average-sized bouton was greater at 30 Hz than at lower frequencies. *E*, the fraction of total bouton area occupied by endosome profiles increased systematically but not significantly ($P > 0.05$) with increasing frequency. Error bars in this and subsequent figures are S.E.M.

bouton area occupied by them (not shown) increased substantially, and then markedly decreased. Time constants for the decrease (single exponential decay) were 12.2 s (number) and 8.3 s (fraction). Thus, while overall dye uptake increased monotonically as endocytosis continued after stimulation (Fig. 5*A*), the dye content of endosomes first increased and then decreased (Fig. 5*B* and *C*). Given that endosomes continued to form after

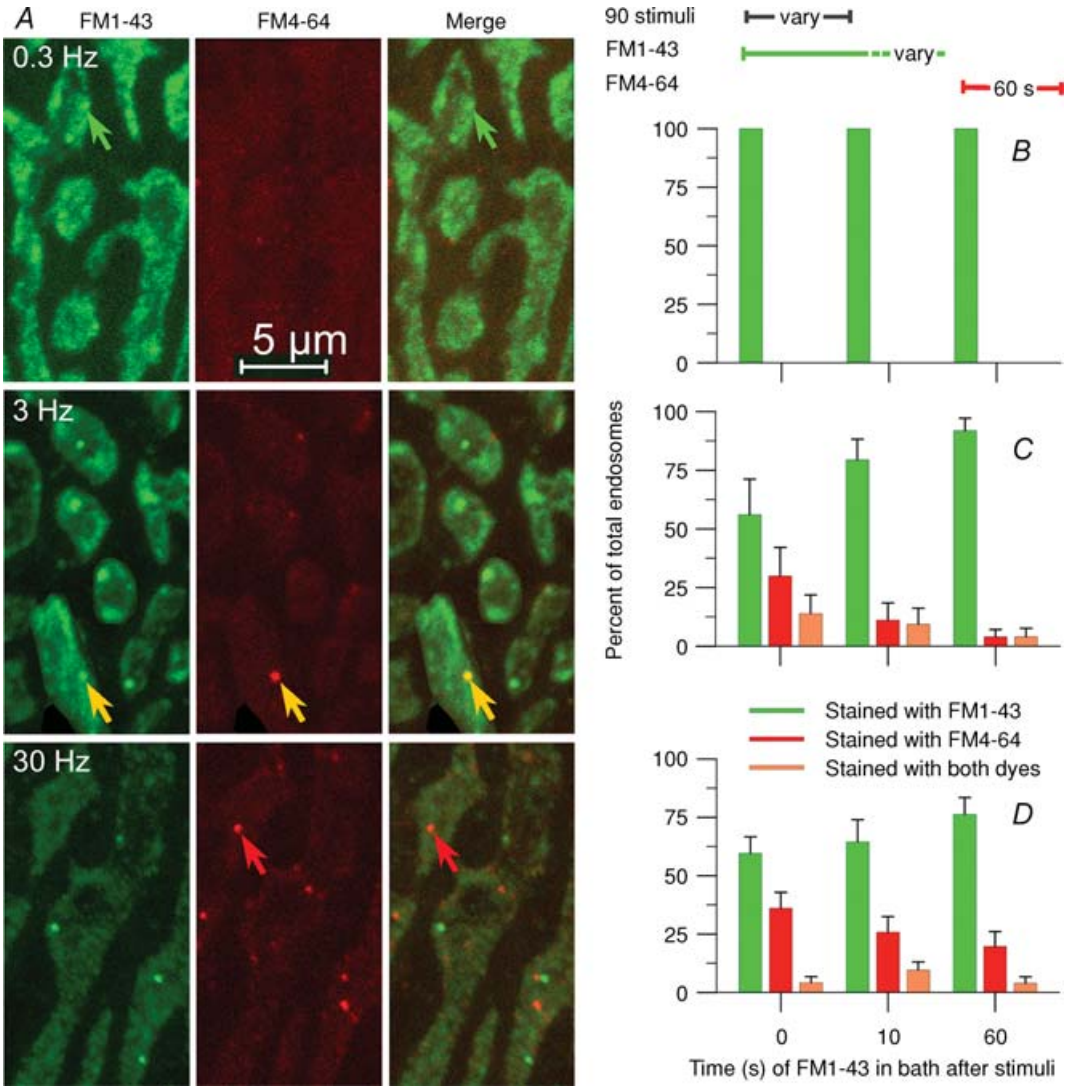

Figure 3. ME occurs both during and after stimulation
Membrane infoldings can remain patent for a time sufficient to internalize two sequentially applied dyes. *A*, nerve terminals received 90 stimuli in an FM1-43 (green) bath at the frequencies indicated, then 60 s rest in an FM4-64 (red) bath. Most endosomes internalized during stimulation, taking up the green dye only (green arrows). Others did so after stimulation, taking up the red dye only (red arrows). A few endosomes infolded during stimulation (retaining dye), remained patent, then internalized during the rest period (yellow indicating both dyes, yellow arrows). *B–D*, percentage of endosomes labelled green (first dye, green bars), red (second dye, red bars) or with both dyes (orange bars) at each of the frequencies shown in *A* (left). The first dye was removed and exchanged for the second either immediately after stimulation (as in *A*), 10 s after stimulation or 60 s after stimulation. *B*, at 0.3 Hz, virtually 100% of ME was completed during the 300 s stimulation. *C*, at 3 Hz, ~56% of endosomes remaining immediately after stimulation were internalized during the stimulation. By 60 s after stimulation, ~92% of endosomes remaining were internalized (green bars). Of the remaining 10%, ~5% had begun forming (infolded) by 1 min after stimulation, but internalized sometime later (orange) and ~5% infolded and internalized between 1 and 2 min after stimulation (red; 60 s time point). *D*, at 30 Hz, only ~75% of endosomes present 1 min after stimulation had internalized during or within 1 min after stimulation. Of the remaining 25%, 20% infolded and formed during the second min (red; 60 s time point) while ~5% infolded by 1 min after stimulation but internalized during the subsequent minute (orange). The prolonged period of endosome formation at high frequency parallelled a similar prolonged period of CME (see text).

stimulation (Figs 3 and 4), we infer that they dissipated into vesicles concomitantly. Data at lower frequencies (0.3 and 3 Hz; not shown) were consistent with this finding, but because most compensatory endocytosis was completed during the stimulus period, it was difficult to separate formation and dissipation of the remaining endosomes in time.

We also examined the formation and dissipation time course using continuous stimulation at 30 Hz. Due to synaptic depression, the need for compensatory endocytosis was greatest initially and then decreased over time. Figure 6*A* shows typical endosomes in preparations stimulated for various durations (9–240 s) in a dye-containing bath, then washed (20 s) and fixed. Image brightness and dye concentration were adjusted to optimally view endosomes. The number of endosomes visibly increased over the first 9 s of stimulation, then decreased. Some endosomes appeared 'fuzzy', starting after ~18 s (arrowheads). Data averaged from all experiments are presented in Fig. 6*B–D* ($n = 356$–775 boutons, 11–23 NMJs, 2–4 snakes per time point). The mean size of endosomes increased until ~36 s, then decreased (Fig. 6*B*). The number (Fig. 6*C*) or total area occupied by endosomes (Fig. 6*D*) increased initially, levelled off at ~18 s, decreased sharply until 36–60 s, then decreased slowly and approached a steady state of 1–2 endosomes per bouton.

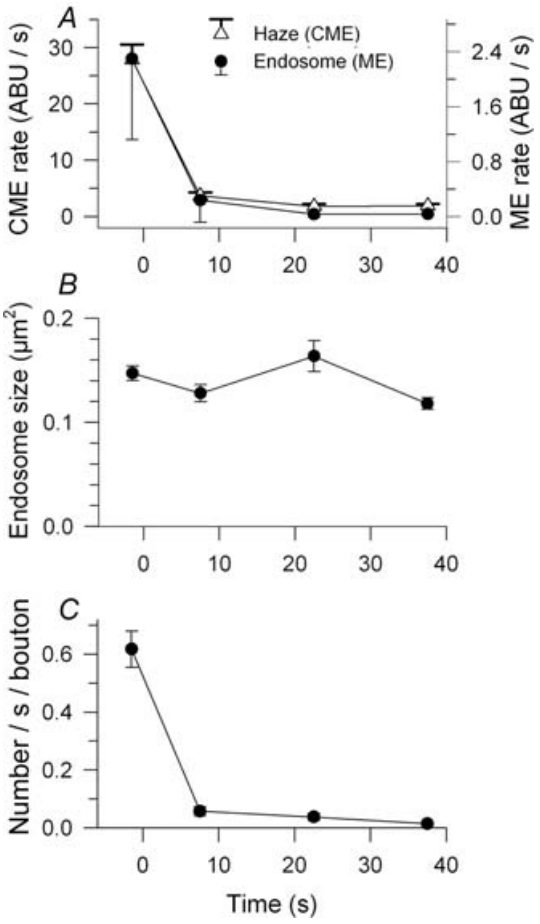

Figure 4. The time courses of ME and CME after a brief high frequency stimulation were similar
A, endocytic rate during (first data point) and subsequent to 30 Hz, 3 s stimulation at times indicated is shown separately for CME and ME. CME contributed far more dye uptake, as measured in brightness increase per unit time (ABU s^{-1}; note separate ordinates with scales normalized so that initial data points overlap). Time course of decay was similar for both endocytic modes. *B*, endosome size did not depend significantly on time of formation. *C*, rate of endosome formation by actual count was similar to rate of ME assessed by FM1 43 brightness.

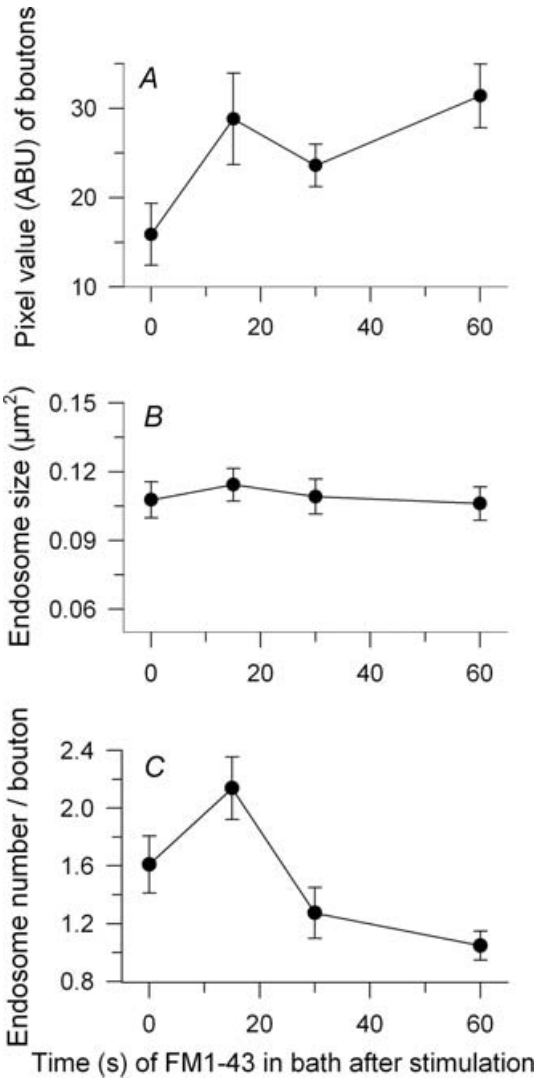

Figure 5. Endosomes formed and dissipated simultaneously after a brief stimulation (30 Hz, 3 s)
FM1–43 remained in the bath until the indicated times after stimulation. *A*, overall dye uptake (average bouton brightness; endosomes plus vesicles) increased after stimulation, approximately doubling by 60 s. *B*, endosome size did not change. *C*, the number of endosomes increased and peaked during the first 15 s after stimulation, then fell.

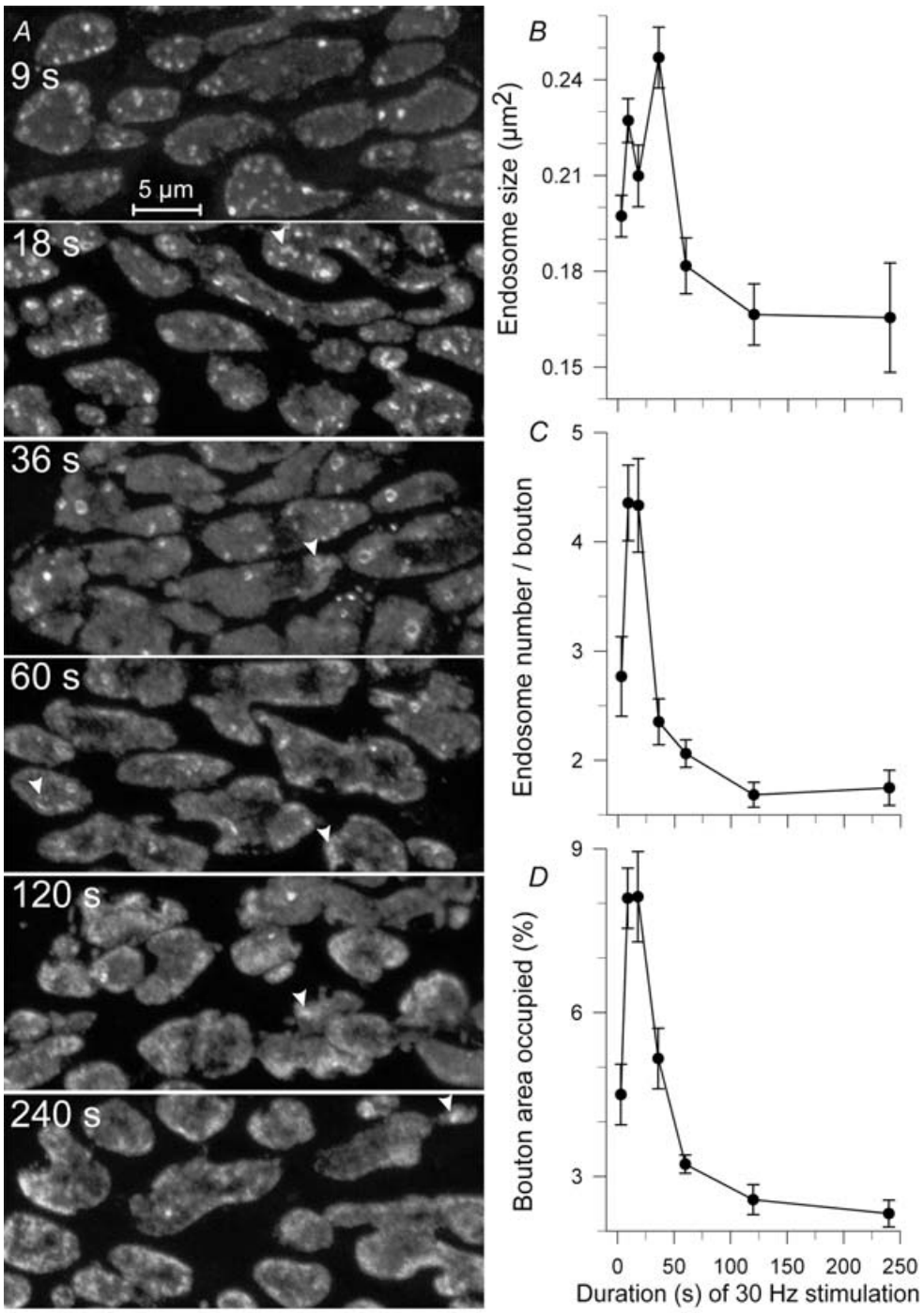

Figure 6. The number of endosomes first rose, then decayed to a steady state during continuous stimulation at 30 Hz

Data points averaged from preparations stimulated in FM1-43 for the times indicated and then fixed. *A*, typical endosomes (punctate spots) and vesicles (haze) internalized at various times during stimulation. Brightness of each image was adjusted to optimize visualization of endosomes. Endosomes contributed substantially to overall brightness initially (1–36 s) but most dissipated over time (60–240 s); those remaining often appeared fuzzy (arrowheads). *B*, mean size of endosomes seemed to increase slightly, then decrease with duration of stimulation (differences not significant). *C* and *D*, mean number of endosomes (*C*) and area occupied (*D*) increased substantially, then decreased with duration of stimulation. A steady state in number and total area was reached at ∼120 s.

The single exponential time constant of the decrease was 24.5 s (number) and 35.1 s (area occupied), longer than the time constants when the preparation rested after a pulse of stimulation (~10 s; Fig. 5).

The decline in number of endosomes during continuous stimulation (Fig. 6*C* and *D*) suggested that most endosomes dissipated. We wondered if those remaining had simply avoided dissipation, or alternatively, if new endosomes had continued to form while older ones dissipated. To answer this question we modified the continuous stimulation experiments of Fig. 6 by beginning stimulation with FM1-43 applied to the bath, and then, after either 18, 60, 120 or 240 s, changing the dye to FM4-64. The latter remained for 60 s at which time we ceased stimulation, washed (20 s) and fixed (Fig. 7). Typical images of terminals where the dye colour was changed at the times indicated are in Fig. 7*A*. Image brightness and dye concentration were adjusted to optimally view endosomes. As in the experiments of Fig. 3, three classes of endosomes were seen: those formed and internalized before the change (FM1-43 only; green arrows), those formed and internalized after the change (FM4–64 only; red arrow) and those that began to form before the dye change but internalized after (both dyes; yellow arrows). Averaged results are in Fig. 7*B–E* ($n = 521$–554 boutons, 14 NMJs, 2 snakes per time point). As in the experiments of Fig. 6, endosome size measurements were scattered, but there was a small systematic decrease over 300 s (~50%), the maximum duration of 30 Hz stimulation studied (Fig. 7*B*). In contrast, the number (Fig. 7*C*) and total area (Fig. 7*D*) of endosomes formed during incubation with FM1-43 decreased sharply and monotonically with time and appeared to be approaching zero. The number of endosomes formed during incubation with FM4-64 decreased also, and nearly reached a steady state of ~1 per bouton. Consequently the total number of endosomes (red + green + yellow) and their total area decreased over time, asymptotically approaching a steady state, consistent with the results of Fig. 6. Within that total number, however, the fraction of endosomes formed before dye exchange (Fig. 7*E*, green bars) decreased, and the fraction of endosomes formed after dye exchange (red bars) increased, as we exchanged dyes at later and later times during the continuous stimulation. The fraction of endosomes containing both dyes was substantial (~10%) and roughly the same regardless of time of dye exchange (Fig. 7*E*, orange bars). Thus, the initial steep decline in endosome number represented dissipation of endosomes formed early on. Eventually, a balance was reached between formation and dissipation. We conclude that the 1–2 endosomes per bouton seen after 3–4 min of stimulation (Figs 6 and 7) represented a dynamic equilibrium between dissipation of older endosomes and formation of new ones.

Endosome dissipation rate is not altered by activity

We stimulated dye-loaded terminals in the absence of dye (destaining) to assess whether the rate of dissipation of endosomes into vesicles is influenced by further stimulation, and whether endosome dissipation limits the rate at which recently endocytosed vesicles are reformed and re-released (Fig. 8). Terminals were loaded with FM1-43 at 30 Hz for 18 s. Each of 10 preparations from one snake was loaded, briefly washed (10 s) and then transferred to a dye-free bath. Five preparations (Destain panels in Fig. 8*A*) were re-stimulated (30 Hz, 5 min) after a delay of 0, 5, 10, 15 or 25 min, respectively, and then fixed. The other five preparations (Stain panels in Fig. 8*A*) were not re-stimulated, but remained in the bath for identical times (5–30 min) before fixation. Results from three sets of experiments ($n = 244$–728 boutons, 8–20 NMJs per data point, 3 snakes) are summarized in Fig. 8*B–E*. The total brightness of control terminals (haze plus endosomes) decreased slightly over 30 min (Fig. 8*B*, filled circles). Destaining of total brightness was slight at 0 min delay, then increased monotonically with increasing delay time (Fig. 8*B*, open circles). The destaining fraction (destaining normalized to control staining at each delay time; Fig. 8*B*, filled triangles) was ~15% with no delay (except 10 s washing time) and ~60% with delay. The requirement of a delay before substantial destaining can occur suggests that recently released vesicle membrane is initially unavailable for re-release, as we have reported (Lin *et al.* 2005). In that study, however, vesicular and endosomal destaining were not separately examined. Interestingly, the size of endosomes appeared somewhat diminished by stimulation (Fig. 8*C*) but their total number (Fig. 8*D*) and total area (Fig. 8*E*) at a given time after the first stimulation were not. Thus, dissipation of endosomes internalized by the first stimulation occurred at the same rate whether or not the preparation was re-stimulated. This rate may limit the number of reformed vesicles available for re-release. At the longest delay, for example (rightmost panels in Fig. 8*A*, and *B*) the vesicular haze was largely destained, with most of the remaining dye appearing within endosomes. This suggests that additional destaining might have been possible had the endosomes dissipated more rapidly.

Endosomes are not responsible for lack of rapid recycling

We performed additional destaining experiments to determine if inability of endocytosed vesicles to be rapidly re-released (Fig. 8*B*) is due to the retention of membrane in endosomes (Fig. 9). Identical loading and destaining protocols were used at two frequencies, 30 Hz ($n = 342$–622 boutons, 8–16 NMJs per data point,

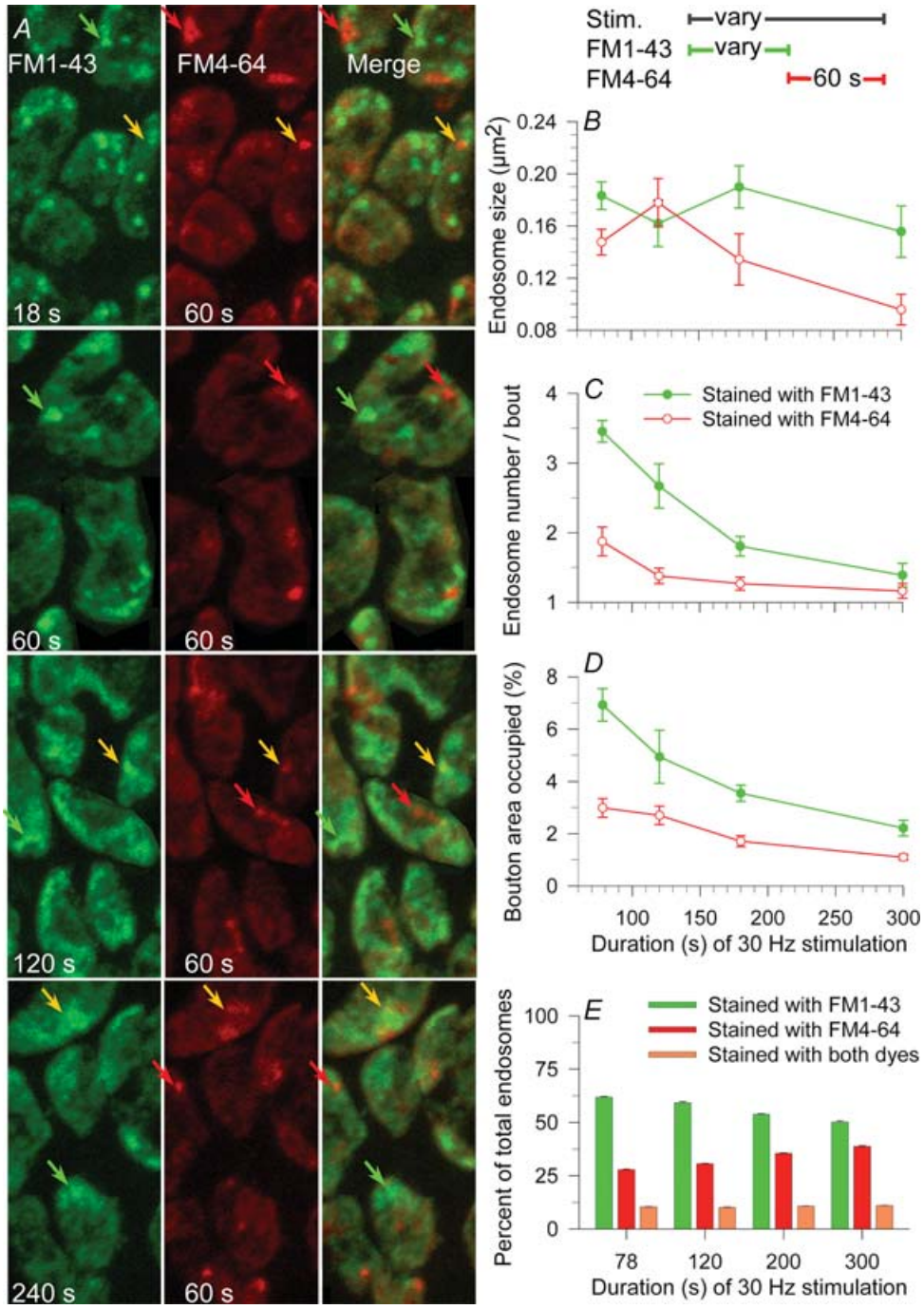

Figure 7. Simultaneous formation and dissipation of endosomes during continuous 30 Hz stimulation
The bath contained FM1-43 (green) until the times indicated and was then changed to FM4-64 (red). *A*, typical boutons imaged after the times indicated in FM1-43, plus 60 s in FM4-64. Brightness of each image was adjusted to optimize visualization of endosomes. Most internalized endosomes contained FM1-43 (green arrows), some contained FM4-64 (red arrows) and some contained both dyes (yellow arrows). *B*, mean size of endosomes did not change significantly with time of stimulation. *C*, as stimulation continued, the number of endosomes formed in the green bath but still remaining after 60 s in the red bath decreased substantially with time, indicating that endosomes formed early on were dissipating (see text). The number of endosomes formed during the final 60 s in the red bath decreased slightly and approached a steady state of ~1 per bouton. *D*, total bouton area occupied by endosomes tracked changes in endosome number. *E*, as stimulation continued, the fraction of total endosomes that had formed earlier but still remained (green) decreased while the fraction of endosomes formed during the last 60 s (red) increased. The fraction of endosomes that were patent during the dye change, and thus contained both dyes, was about 10% regardless of stimulus duration (orange).

2 snakes) and 1 Hz ($n = 541$–762 boutons, 16–17 NMJs per data point, 2 snakes). Stimulation at 30 Hz was for 18 s (same as loading stimulation in experiments of Fig. 8). The dye remained in the bath for an additional 60 s (sufficient for completion of endocytosis) before washing (10 s). Control preparations were allowed to rest either ∼5 min (short delay) or ∼33 min (long delay) before fixation. Destain preparations were re-stimulated either 110 s after wash (short delay; 2 min after stimulation; to attempt rapid recycling) or after 30 min rest (long delay). To confirm that NMJs had fully recovered from depression before re-stimulation at short delay, we reversed staining and destaining in an additional control, first stimulating in dye-free solution and then loading. Typical examples of partial labelled terminals from each protocol are in Fig. 9*A*. Timing details of protocols are directly above each image. Staining intensity was similar in control terminals for both short delay (Control S) and long delay

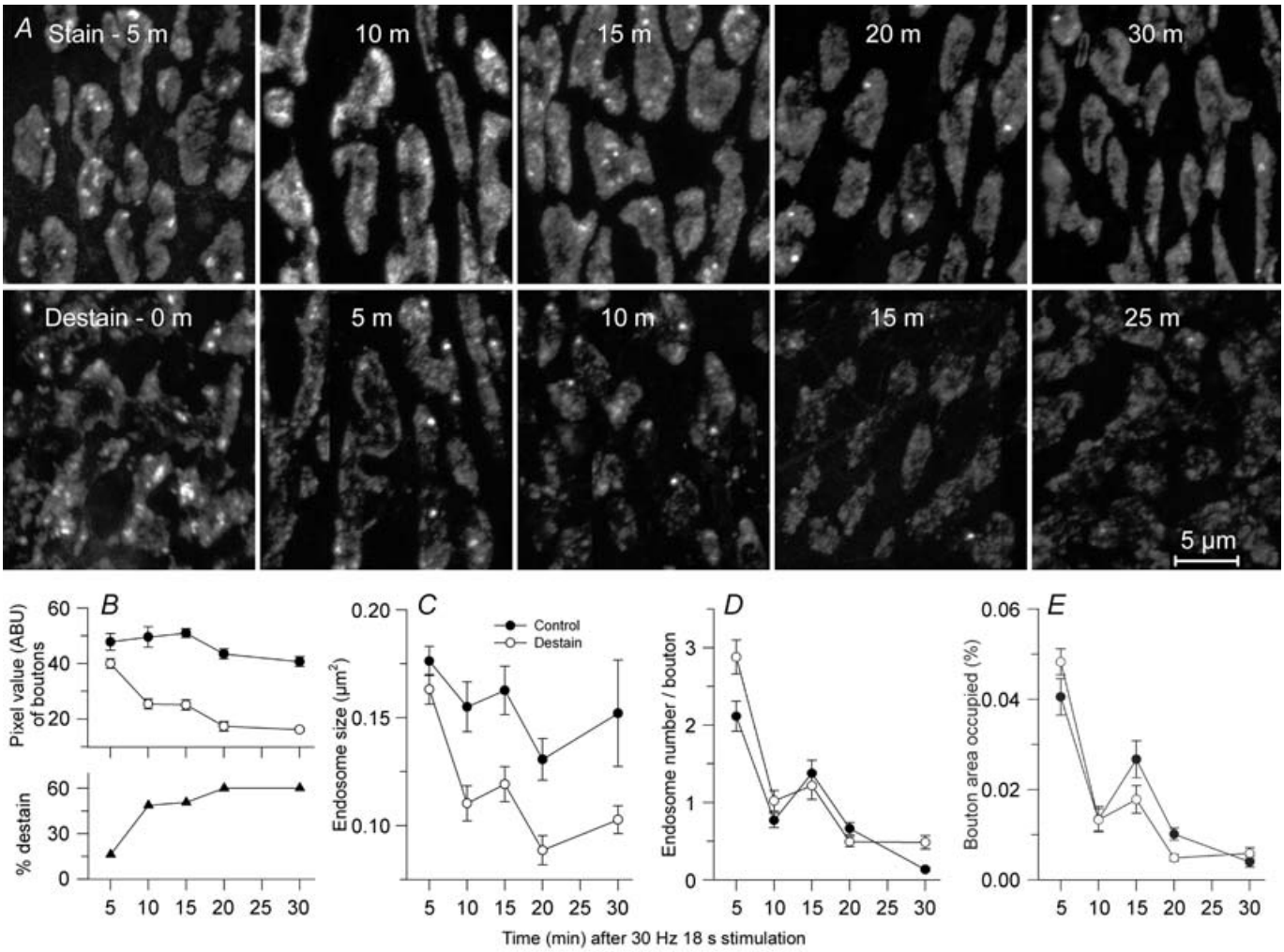

Figure 8. Activity has no effect on endosome dissipation
Terminals were loaded with dye (30 Hz, 18 s), washed (10 s), rested for various times, then restimulated (destained; 30 Hz, 5 min) at the times after loading indicated and immediately fixed. Control terminals were loaded with dye and rested for identical total times before fixation. *A*, portions of example terminals. Staining intensity of control terminals (Stain) decreased slightly with increasing delay time; note dissipation of endosomes, which was nearly complete at 30 min. Restimulated terminals (Destain) destained only slightly at the shortest delay, but destained substantially at longer delays (see Fig. 9). Destaining was due primarily to loss of vesicle haze; note bright endosomes remaining. *B*–*E*, averaged data from all experiments. *B*, destaining after various delays (▲) was taken as $(C - D)/D$ where C is brightness of control boutons (■) and D is brightness of destained boutons (○). *C*, endosomes ranged in size and data were scattered. Those in destained terminals may have been somewhat smaller than those in controls. *D*, destaining did not alter the dissipation rate of endosomes formed previously. The number of endosomes still remaining decreased exponentially with time whether or not the terminal was restimulated. *E*, decrease with time of bouton area occupied by endosomes (number × size) was also insensitive to stimulation.

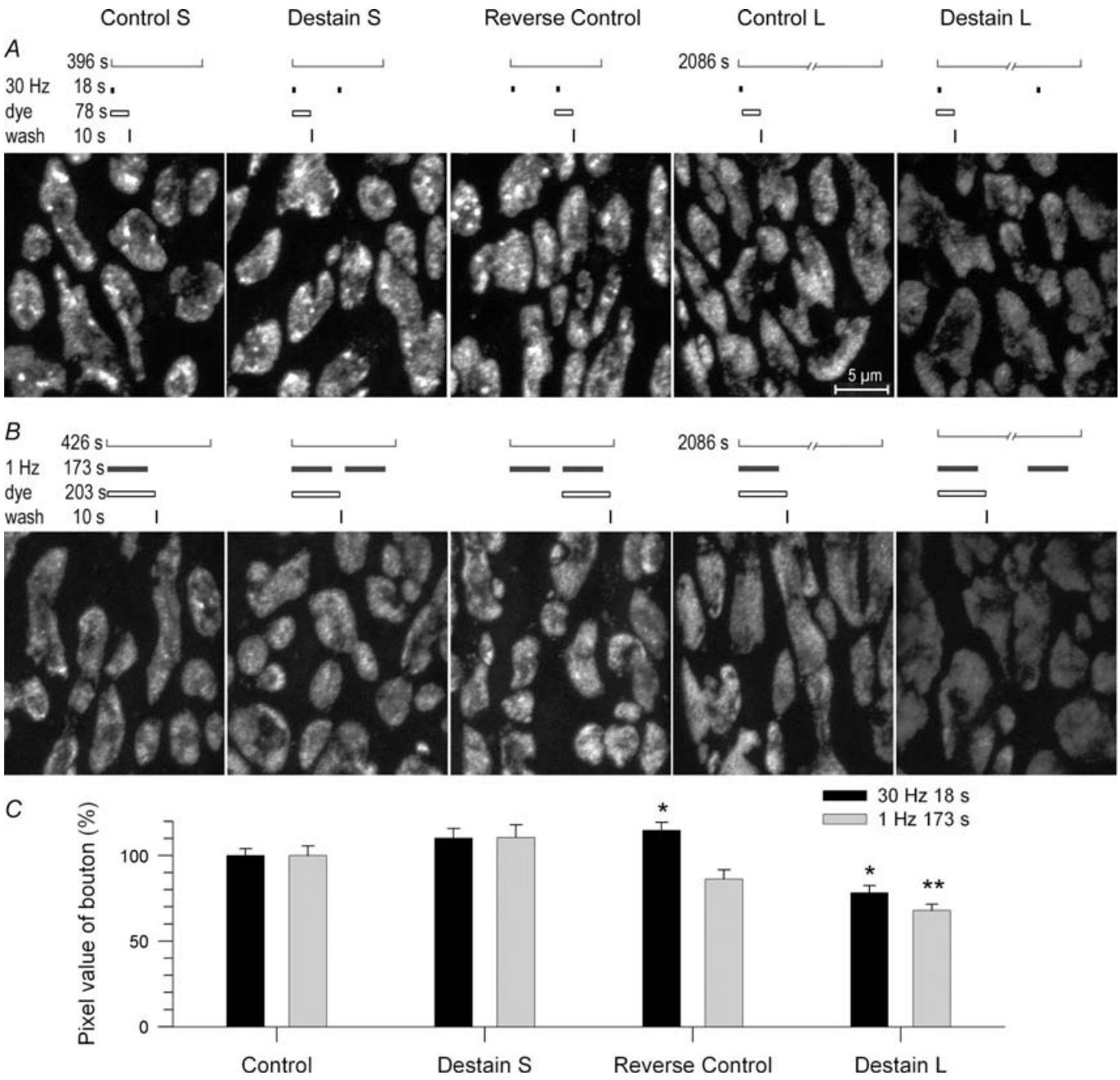

Figure 9. Endosomes were not responsible for lack of rapid recycling
A and *B*, terminals were loaded with FM1-43 at either high (30 Hz, 18 s) or low (1 Hz, 173 s) frequency and then restimulated with the identical stimulations delivered after either short delay (Destain S; 290 s) or long delay (Destain L; ∼30 min). Control terminals (S or L) were loaded and allowed to rest before fixation at the same time as restimulated terminals. Reverse control terminals were stimulated without dye, then restimulated with dye (short delay only; see text). The loading/destaining protocol that corresponds to each example image is shown above it. *A*, example partial terminals at 30 Hz. Note labelled endosomes in all preparations restimulated after a short delay, but not in those restimulated after a long delay. *B*, example partial terminals at 1 Hz. Note virtual absence of labelled endosomes in all protocols. *C*, summary of data from all experiments; dye brightness of controls normalized to 100%. Control, short delay, and reverse control terminals did not differ significantly in dye uptake, with the exception of the 30 Hz reverse controls, which took up slightly but significantly more dye with the second stimulation than with the first. Long delay terminals destained 20% (30 Hz; $P < 0.05$) and 30% (1 Hz; $P < 0.01$). Many recently endocytosed vesicles (haze) were available for release after the short delay (Control S) as after the long delay (Control L).

(Control L). Both sets of control terminals contained labelled vesicles appearing as haze. Short delay controls contained endosomes while long delay controls contained virtually none, presumably because they had dissipated during the delay period. Re-stimulation beginning after the short delay did not visibly destain terminals (Destain S) whereas re-stimulation after the long delay did (Destain L). Dye uptake during a second stimulation, delivered after a short delay (Reverse control), was similar to uptake during the first (Control S), confirming that preparations had recovered from possible depression during the short delay period. Results averaged from all data (Fig. 9*C*) confirmed that destaining with long delay was successful ($P < 0.05$) whereas attempted destaining with short delay was not.

We specifically noted that vesicle haze did not diminish with attempted destaining after short delay – many recently endocytosed vesicles were present (Fig. 9*A*), but the terminal released unstained vesicles exclusively. Endosomes formed during the loading stimulation were also present (Fig. 9*A*), but there was no evidence that sequestration of membrane in endosomes caused destaining to fail.

As rapid recycling has been particularly associated with low frequency stimulation, we repeated the experiments described above at 1 Hz. We determined separately that 173 stimuli delivered in 173 s released on average the same number of quanta (in normal Ca^{2+} bath) as did the 30 Hz protocol above. Dye remained in the bath for 30 s after stimulation, followed by a 10 s wash. Thus, in addition to equal transmitter release, there were virtually equal times from the beginning of staining to the beginning of destaining (3.5 min for short delay, ∼31 min for long delay) at both frequencies. Results at 1 Hz (Fig. 9*B*; all panels shown at actual brightness) were similar to those at 30 Hz. Again, all three controls (Control S, Control L, Reverse Control) showed similar dye uptake (Fig. 9*B* and *C*). There was no destaining after the short delay (Destain S) but significant ($P < 0.01$, Fig. 9*C*) destaining 30 min after the long delay (Destain L). Thus, at either frequency, terminals used exclusively vesicles from the reserve pool, rather than re-releasing those that had been recently endocytosed.

EM study of endosomes

We used three stimulation protocols, identical to those in the optical studies of Fig. 2 except that HRP was the endocytic marker. All studies utilized serial sections (3–41 sections per series; 413 sections at 0.3 Hz, 262 sections at 3 Hz, 423 sections at 30 Hz). The number of boutons studied was 20 at 0.3 Hz, 17 at 3 Hz, and 32 at 30 Hz. Figure 10 shows 3-D stereo pairs of partial boutons reconstructed from serial EM sections (two flyover movies are available in the online Supplemental material version). The underlying postsynaptic membrane (blue) and capping Schwann cell membrane (purple) indicate the orientation of each partial bouton. The example for 30 Hz stimulation contains parts of two small adjacent boutons. Labelled structures that appeared in only one thin section are depicted as white, while those (larger) structures that crossed more than one section are shown red. Labelled structures were more numerous when 90 stimuli were delivered at 0.3 and 3 Hz than at 30 Hz (9.90, 8.19 and 2.58 structures per section, respectively; see Fig. 14). This was consistent with the higher FM1-43 staining intensity seen at the lower stimulus frequencies (Fig. 2*B*), due to depression of release at the higher frequency. Structures appeared dispersed throughout the

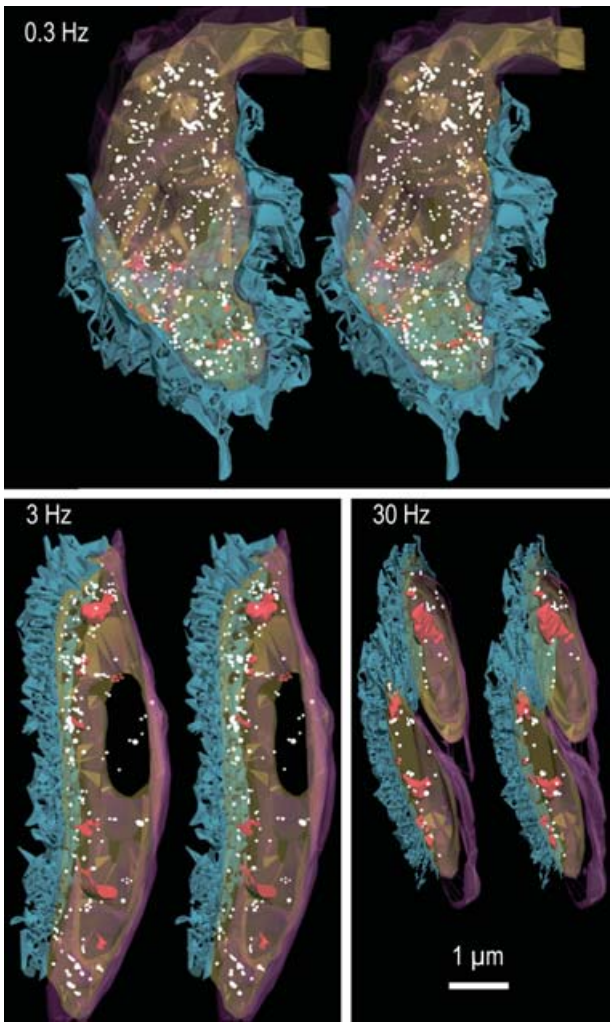

Figure 10. Reconstructions (13–40 serial sections) of example partial boutons loaded with HRP via 90 stimuli delivered to the muscle nerve at the frequencies indicated
Vesicles (white) and endosomes (red) appear throughout the boutons although many remain near the presynaptic membrane (grey). Postjunctional folds (blue) appose the presynapse while Schwann cell processes (purple) cap the boutons. Stereo pairs are for viewing with eyes uncrossed.

boutons regardless of stimulation protocol, although more of them had moved inward from presynaptic membrane (yellow) at lower frequency and longer duration (see Fig. 14). We describe below four types of labelled structures: vesicles, large (macro) endosomes, clusters of small endosomes, and membrane infoldings (Figs 11–13). Structures smaller than 0.005 μm^2 area ($<$ 70 nm diameter) are referred to as vesicles. They were similar in size to unlabelled vesicles, were usually found in a single thin section, and were often coated with clathrin, apparently budding either from endosomes or from the presynaptic membrane.

We saw large endosomes (hundreds of nanometres in diameter) at all stimulus frequencies. Examples are in Fig. 11. Typical shapes are shown in the 3-D renderings of Fig. 11*A*; the individual serial sections can be appreciated by slight changes in contrast among the stacked 'slices.' Endosomes were usually C-shaped but sometimes closed or nearly so, as in the example at 0.3 Hz. As in other species, their surface area-to-volume ratio was maximized (like a ball emptied of air), presumably to minimally alter the bouton's volume. Figure 11*B–D* shows example EM sections from the renderings of Fig. 11*A*; each section corresponds to the 'slice' marked by an asterisk in the rendering above it. Other example EM sections containing portions of endosomes are in Fig. 11*E–H*. Coated vesicles apparently budded from the endosomes (arrows) and coated vesicles in the process of budding (arrowheads) were common. Rapid budding of vesicles from large endosomes, particularly at 30 Hz stimulation, was consistent with the rapid phase of endosome dissipation seen at light level.

Small endosomes varied in size – some no larger than two vesicles. They were seen near large endosomes, and occasionally near infoldings (see Fig. 13*A*), clustered with each other and with labelled vesicles (Fig. 12). Renderings (Fig. 12*A*) suggest that each cluster had split from a common precursor (Discussion). An example section from each rendering is shown directly below (Fig. 12*B–D*). In individual sections, coated vesicles were often seen budding (arrowheads) or apparently budded (arrows) from the small endosomes (Fig. 12*B–H*) just as they did from large ones. Among all endosomes (large and small) 70% were seen budding at 0.3 Hz, 48% at 3 Hz, and 41% at 30 Hz. Endosomes in clusters were observed mostly in 0.3 Hz preparations (91% in clusters, 9% solo) but also at 3 Hz (38% clustered, 62% solo) and 30 Hz (6% clustered, 94% solo) as well.

Membrane infoldings were seen at all frequencies (1 at 0.3 Hz, 2 at 3 Hz, 110 at 30 Hz). They retained HRP

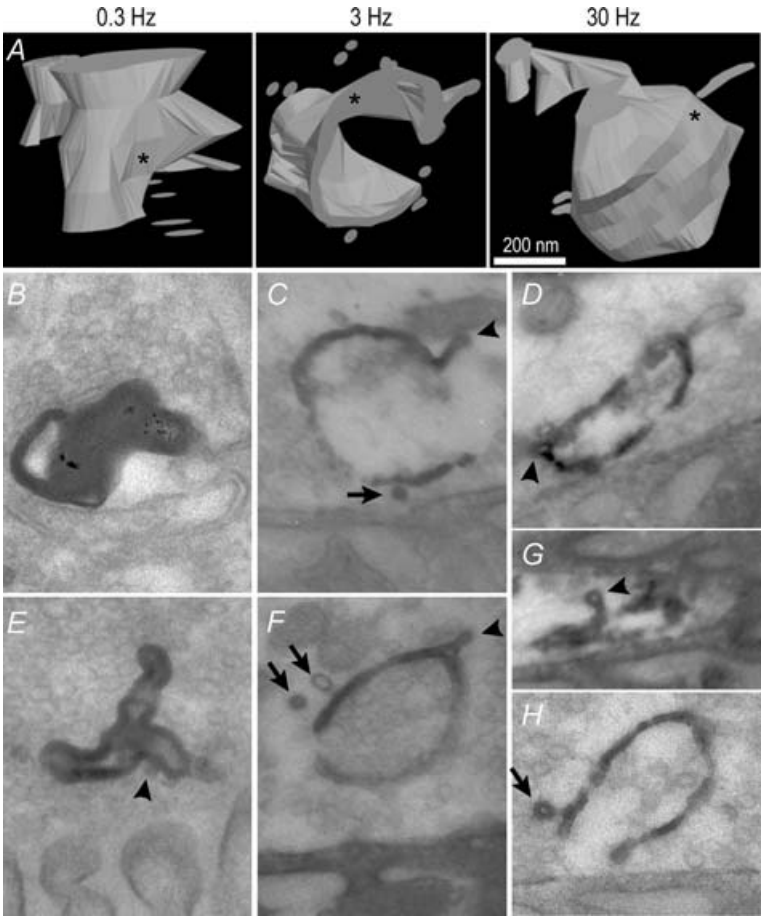

Figure 11. Endosome ultrastructure was similar at all stimulation frequencies
A, example renderings of large (macro) endosomes seen in preparations loaded with HRP as in Fig. 10. Each rendering comprises 6–15 serial sections. Nearby labelled vesicles were found in single EM sections and are shown as disks. *B–D*, example sections corresponding to those marked by asterisks in the renderings directly above. *E–H*, other examples of individual sections containing macroendosomes. Arrows point to clathrin-coated vesicles. Arrowheads point to putative budding vesicles.

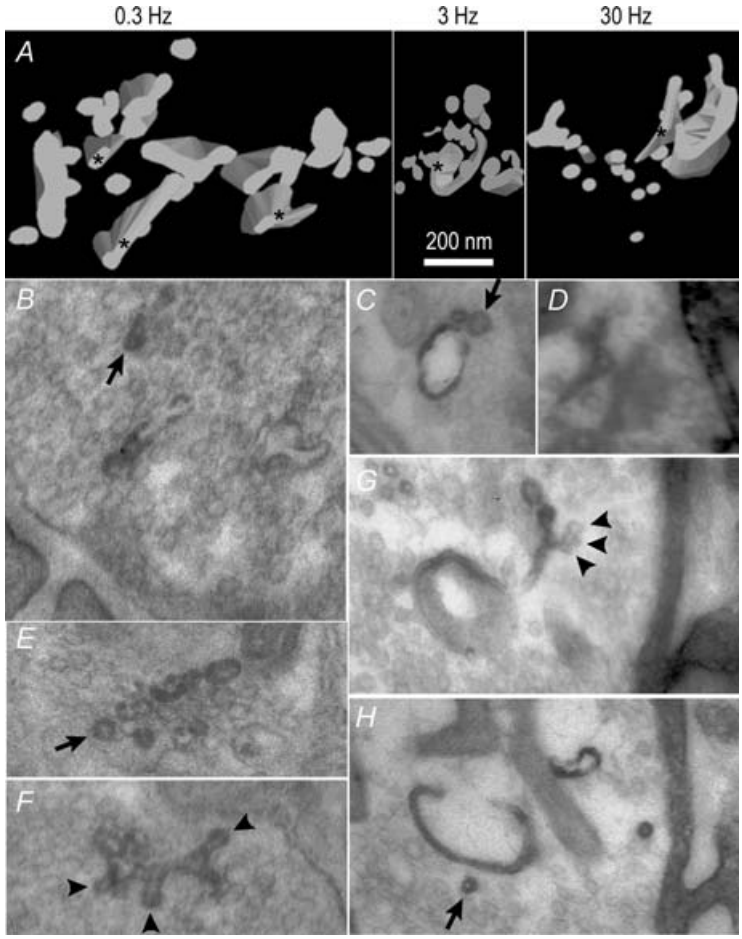

Figure 12. Small endosomes appeared in clusters
A, example renderings of small endosomes seen in preparations loaded with HRP as in Fig. 10. Each rendering comprises 4–7 serial sections. *B–D*, example sections corresponding to those marked by asterisks in the renderings directly above. *E–H*, other examples of individual sections containing pieces of clusters. Arrowheads point to clathrin-coated vesicles while arrowheads point to putative budding vesicles.

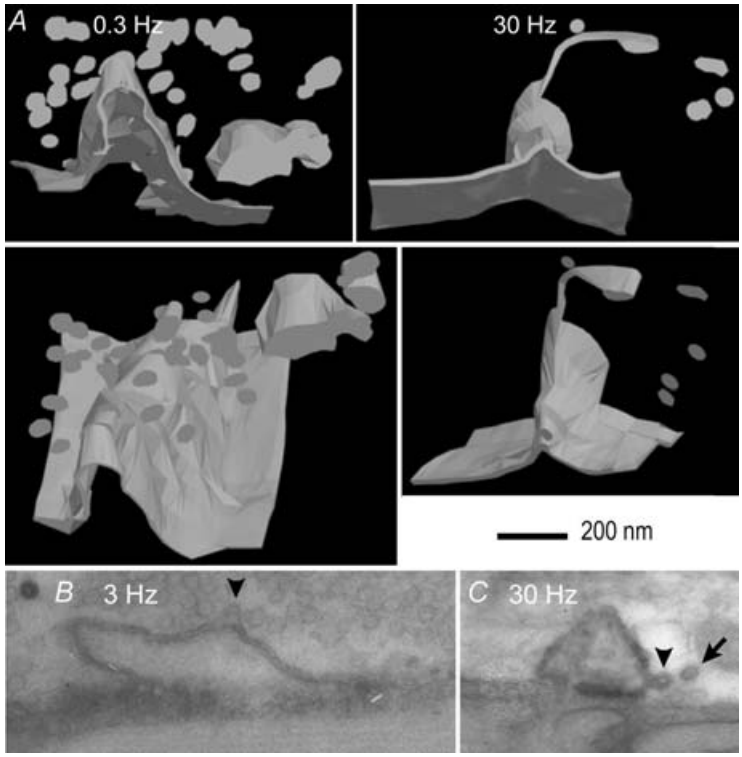

Figure 13. Precursor membrane infoldings budded vesicles before fisson was complete
A, example renderings of membrane infoldings depicted from outside (above) and inside (below) the bouton. Renderings comprise 17 serial sections (0.3 Hz) and 6 serial sections (30 Hz). HRP loading protocol as in Fig. 10. Note coated vesicles (disks) that appear to have budded from the infolding. *B* and *C*, examples of vesicles apparently budding (arrowheads) and budded (arrow) vesicles from the infoldings as seen in individual sections.

to varying extents, probably because of variability in rinsing. Presumably, some or all would have progressed to fully internalized endosomes had the process not been interrupted by fixation. Two examples are presented in the 3-D renderings of Fig. 13; each is depicted (above) as viewed from the cleft and (below) as viewed from within the bouton. Most infoldings were undergoing clathrin-mediated vesicles budding at the time of fixation (all 3 infoldings seen at lower frequencies; 64% at 30 Hz; arrowheads; Fig. 13*B* and *C*) or had already budded vesicles (arrow).

We compiled the size and distribution of HRP-labelled structures seen in individual EM sections (Fig. 14). The size distribution of structures was similar at all frequencies (Fig. 14*A*). Most were vesicles. Larger structures (endosomes) were less numerous as their size increased. The percentage of total labelled structures of any particular size depended systematically upon stimulus frequency (Fig. 14*B*). Vesicles were relatively more abundant at 0.3 Hz while endosomes were more abundant at 30 Hz, consistent with data at light level (e.g. Fig. 2).

We found previously that CME occurs near AZs, which appose postsynaptic folds (Teng & Wilkinson, 2000). To assess movement of labelled structures after their internalization we therefore measured each structure's distance from the nearest fold opening. Vesicles (Fig. 14*C*) and endosomes (Fig. 14*D*) were separately analysed. While there were more labelled vesicles closer to fold openings

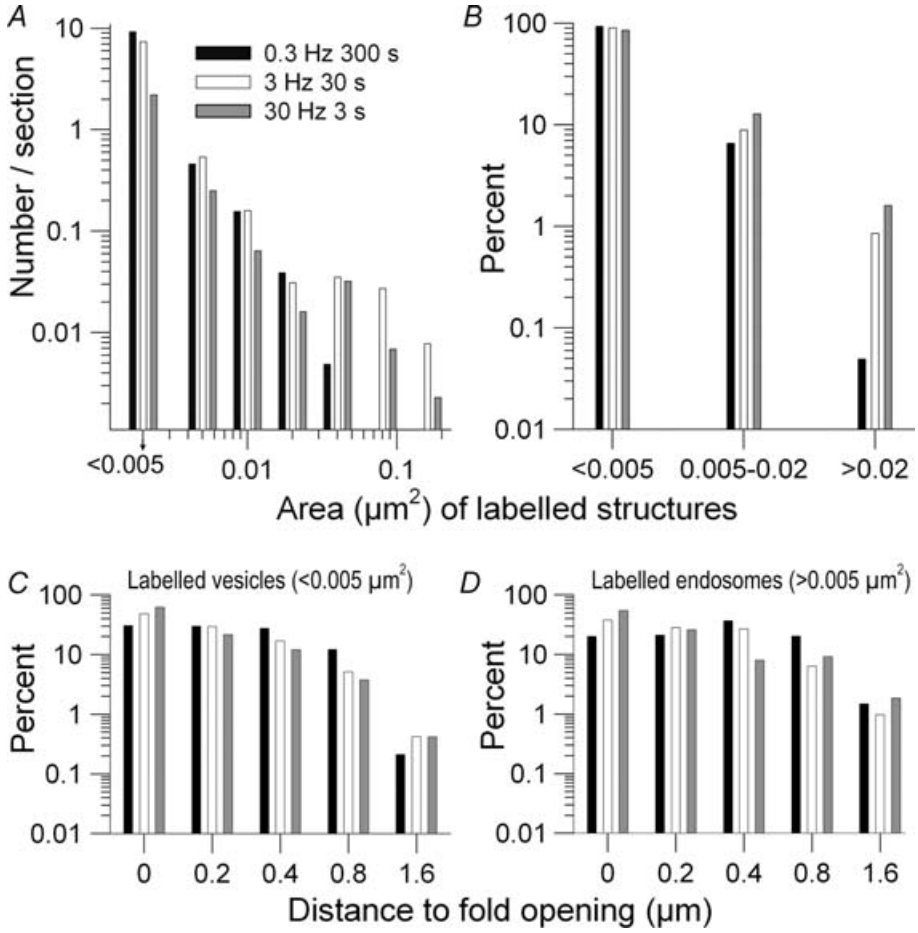

Figure 14. Size and location of labelled endocytosed structures seen in *xxy* sets of serial EM sections (69 sets, 3-40 sections per set) after 90 stimuli delivered at three frequencies
A, histogram of structure sizes (area; $< 0.005\ \mu m^2$ are vesicles). When a structure appeared in two or more serial sections, only the largest section of the structure was counted. A continuum of structure sizes was observed at all frequencies, including some no larger than two or three vesicles combined. Smaller structures were far more prevalent than large ones (note logarithmic ordinate in all histograms). *B*, percentage of total structures in three size ranges: vesicles, small endosomes and large endosomes. The majority of endocytosed structures were vesicles. With increasing frequency, the relative prevalence of endosomes increased while the relative prevalence of vesicles decreased. *C* and *D*, similar distributions of labelled vesicles (*C*) and endosomes (*D*) within boutons. Both structures tended to randomize their positions by moving away from the membrane into the vesicle pool. The randomization was most complete after 300 s at 0.3 Hz, and least complete after 3 s at 30 Hz.

(and hence the plasma membrane), many vesicles clearly moved towards the bouton's centre. Movement was most evident at 0.3 Hz – vesicles were nearly equally distributed over a distance of nearly 1 μm from the membrane – essentially the entire region available to vesicles outside of the mitochondria-rich bouton core. At higher frequencies, vesicles had not moved inward as much. Endosomes (Fig. 14*D*) behaved similarly to vesicles. After prolonged low frequency stimulation they were uniformly distributed, while after brief high frequency stimulation they were found closer to the membrane.

Discussion

At both light and EM levels, we have shown that compensatory membrane retrieval is shared by ME and CME over two decades of stimulation frequency. ME contributed substantially, and in about the same proportion relative to CME, at all frequencies. Our findings differ substantially from previous reports that describe the role of endosomes in synaptic vesicle recycling. Specifically, dissipation of endosomes into vesicles was very fast, and we found no evidence for any direct change in endocytic strategy with change in stimulus protocol.

Endosomes form rapidly and are present at all levels of use

Endosomes formed in 3 s (30 Hz), the shortest stimulation time which gave consistent results. In five preparations stimulated at 30 Hz for 1 s, two contained endosomes and three did not (data not shown). Preparations fixed after 3 s always contained endosomes visible at both light and EM levels. Thus, at least for some endosomes, internalization required at most 1–2 s. Our two-dye experiments also suggest that times around 1–2 s are reasonable. During continuous stimulation (Fig. 7), or after stimulation (Fig. 3) when one dye was quickly exchanged for another of different colour, ~10% of endosomes present after fixation contained both dyes (range, 4–14%; see Figs 3 and 7). This means that infoldings capable of retaining dye had formed during application of the first dye, and internalized to become endosomes during application of the second. Thus they remained open at least long enough to allow diffusion of the second dye into the cleft. Similar time constants for formation of endosomes have been reported in other nerve terminal preparations including the rat calyx of Held (1–2 s; Wu *et al.* 2005), and the goldfish retinal bipolar terminal (1–2 s; von Gersdorff & Matthews, 1994; Heidelberger, 2001).

Bulk retrieval of plasma membrane has been considered activity dependent, occurring only after a period of high frequency stimulation (reviewed by Royle & Lagnado, 2003; Rizzoli & Betz, 2005). However, we detected endosomes using FM1-43, high MW dextran and HRP at 0.3 Hz as well as 3 Hz and 30 Hz stimulus frequencies. In addition, endosomes continuously formed, though at a low rate, under severely depressed neurotransmission during prolonged (300 s, the maximum tested) 30 Hz stimulation. Thus, ME was employed at low as well as high levels of use.

In response to endocytic 'debt' during and up to 1 min after a short burst of 30 Hz stimulation, endosomes formed at about the same rate as did vesicles directly budding from presynaptic membrane. Conversely, both types of endocytosis ceased immediately after a 0.3 Hz stimulation over 300 s. ME paralleled CME at all frequencies, and thus seemed not to be triggered by the need for additional membrane retrieval as stimulus rates exceed the capability of CME (e.g. de Lange *et al.* 2003). Rather, it seemed to be triggered along with CME. This behaviour may be similar to that described at the mammalian calyx of Held which undergoes rapid (1–2 s), Ca^{2+}-dependent, clathrin-independent endocytosis during intense nerve activity (Wu *et al.* 2005). Other preparations are reported to trigger ME and CME independently. Endosome formation is the preferred mode of compensatory endocytosis in the goldfish retinal bipolar ribbon synapse, regardless of stimulus duration (Paillart *et al.* 2003). Some motor terminals of *Drosophila*, in contrast, exhibit no bulk endocytosis at all (Koenig & Ikeda, 2005). At the frog NMJ, ME occurs after CME in an activity-dependent fashion (Richards *et al.* 2000). It is possible that different synapses employ different strategies for endocytosis.

Endosomes dissipate rapidly into vesicles

The process of clathrin-mediated budding from endosomes was similar at all stimulus frequencies. In EM sections we saw numerous examples of coated pits and coated vesicles associated with endosomes. Budding began even before endosomes were fully internalized, together with budding directly from the plasma membrane (not shown). Thus, clathrin adapter proteins seemed not to distinguish between plasma membrane that remained apposed to the synaptic cleft and plasma membrane that was internalized, or in the process of internalization.

Vesicle budding from endosomes has been previously observed (Takei *et al.* 1996; Gad *et al.* 1998; Richards *et al.* 2000; Teng & Wilkinson, 2000; Paillart *et al.* 2003) but not characterized in detail. We created endosomes via a short burst of 30 Hz stimulation, and observed an approximate single-exponential decay in number and total area, with time constants of 12 s and 8 s, respectively. Most endosomes therefore dissipated more slowly than they formed (~10 s *versus* ~3.5 s time constant after stimulation burst), but still in the order of seconds, not minutes as reported for other synapses (e.g. de Lange *et al.* 2003; Richards *et al.* 2003).

Dissipation of endosomes into vesicles was via two mechanisms: direct budding and fission of endosomes into clusters of a few smaller endosomes, from which vesicles budded. These small endosomes were below light level resolution, but clusters of them may have corresponded to the fuzzy, irregularly shaped structures described in Results. For example, after 300 s at 0.3 Hz, relatively few endosome-like structures remained, but most of them appeared fuzzy at light level, or as small endosome clusters in EM (91%; Figs 10 and 12). We noticed that most structures imaged at longer times were fuzzier than those imaged at shorter times with 30 Hz stimulation as well (Figs 1, 6 and 7). In EM serial sections, a cluster of small endosomes was sometimes in the vicinity of a large endosome. Also, pieces (larger than a vesicle) sometimes extended from an endosome, either breaking off or still connected. Some large endosomes exhibited a complex geometry consistent with the shape and distribution of clusters – again suggesting that the large endosomes were precursors to the clusters. The prevalence of small endosome formation – rather than direct budding of vesicles from large endosomes – was evident in the distribution of sizes among endocytosed structures (Fig. 14). We observed a continuum of sizes, not a bimodal distribution comprising endosomes plus vesicles, as we had expected. We cannot rule out that some small endosomes entered the terminal via small invaginations directly from the membrane. To our knowledge, endosome clusters of this type have not been previously reported in nerve terminals.

The initial rapid dissipation of most endosomes helped to quickly replenish synaptic vesicles. In contrast, at the frog NMJ (Richards *et al.* 2003) and the mammalian caylx of Held (de Lange *et al.* 2003), the number of synaptic vesicles slowly increases while the number of endosomes decreases for up to 15–30 min after stimulation. Interestingly, the rate of endosome dissipation was not only rapid but unaffected by stimulation. Endosomes formed during and immediately after a first stimulation dissipated at the same rate when the preparation was rested as when it was stimulated a second time.

Destaining required a delay, indicating that reserve pool vesicles were used preferentially to recently endocytosed ones, even at low frequency (also see Lin *et al.* 2005), precisely opposite the behaviour reported for frog (Richards *et al.* 2003; see also Wilkinson & Lin, 2004). The need for a delay was not, however, due to the slow dissipation of some endosomes, as the reserve pool of vesicles in the snake NMJ contained many labelled vesicles that were selectively avoided by the release mechanism. Instead, the delay must be due to some other factor such as time required for vesicle acidification and refilling, or mobilization time to the AZ. We note, however, that even after recycled vesicles gained competence for re-release, a few endosomes remained. The slow tail of endosome dissipation lasted 15 min or more (Fig. 8; see below). This membrane was not yet available to form vesicles, and might therefore limit transmitter release at high levels of use.

Dynamics of ME processing at low and high frequencies

At 0.3 Hz, the 3.3 s interval between stimuli may be sufficiently long to complete both CME and ME after each stimulus. Consistent with this, we detected no dye uptake immediately after 300 s of stimulation. Moreover, dissipation of endosomes proceeded so rapidly ($\sim$10 s time constant) that numerous small endosome clusters and labelled vesicles, but only a few large endosomes in total, were seen in EM preparations fixed after 0.3 Hz stimulation. Thus, there was relatively little membrane sequestered in endosomes (and therefore unavailable to reform vesicles) at this frequency.

The situation at high frequency (e.g. 30 Hz) was known in advance to differ in two ways: initial high but subsequent low need for compensatory endocytosis is required due to depression in release, and endocytic 'debt' occurs after even brief (3 s) stimulation. Thus, we were not surprised to observe a balance between formation and dissipation of endosomes during continuous 30 Hz stimulation (Figs 6 and 7). Initial formation of endosomes was robust (4–5 endosomes per bouton in < 9 s), then declined (2 per bouton), and subsequently equilibrated at $\sim$1 per bouton. Concomitantly, dissipation of endosomes was also initially robust (25–35 s), but then quite slow, also reaching $\sim$1 per bouton at $\sim$120 s of the long stimulation. Endosomes formed and dissipated with single exponential time courses in response to a burst of stimulation as well. Endosome processing at high frequency – formation of new endosomes while older ones dissipated – was so rapid that reformed vesicles could be created in adequate supply for release, just as at low frequency. As proof, little membrane was sequestered in endosomes at 30 Hz, while vesicular haze was abundant. Release, albeit depressed compared with release at low frequency, was not rate-limited by endosome processing. We conclude that the increase in number of endosomes seen with increasing frequency in our 90-stimulus protocols is consistent with an expected greater backlog of membrane, including that of endosomes, awaiting dissipation into vesicles. We found no evidence in any of our experiments for a direct change in endocytic strategy with change in stimulus protocol.

The approximate single-exponential time course of endosome dissipation (rapid initial rate, followed by a slow tail) suggests that the amount of endosomal membrane determined its own rate of dissipation over time. Were some other reactant rate limiting (e.g. clathrin), one would expect a more linear decrease in endosomal membrane

with time. While the slow tail we observed is consistent with this single process, it is also possible that the later stage of dissipation is due to protein sorting, which may employ different mechanisms from the early rapid budding. For example, some endosomal membrane might fuse with the plasma membrane, or enter a degradation pathway.

Reserve pool recycling occurs at all stimulus frequencies

Coated vesicles internalized from the plasma membrane near AZs (and thus seemingly poised for local recycling; Teng & Wilkinson, 2000) did not remain near the membrane for re-release but instead became randomly distributed, with a substantial fraction mobilized inward among unlabelled vesicles of the reserve pool. This random mixing occurs in frog as well (Rizzoli & Betz, 2004). However, in frog, low level stimulation causes such vesicles to be recognized, transported to AZs and preferentially re-released without use of endosomal intermediates (rapid recycling, Richards *et al.* 2003; see also Wilkinson & Lin, 2004). In contrast, we found no evidence for rapid reuse. We used staining and destaining stimulations at high (30 Hz, 18 s) or low (1 Hz, 173 s) frequency that were designed to release ∼20% of the vesicles in the reserve pool. With a long delay (∼33 min), 20–30% of fluorescence was lost by a destaining stimulation. This indicated that vesicles formed a half hour earlier were randomly chosen for release from among all reserve pool vesicles. However, with a short delay (∼2 min) there was virtually no destaining at all. Thus, consistent with a previous report (Lin *et al.* 2005), dye that was internalized a few minutes earlier had lower (near zero), not higher, probability of re-release than unlabelled vesicles in the reserve pool. Here, we add that inability to destain is not because recently internalized membrane is sequestered in endosomes. Most endosomes dissipated fast enough so that their membrane was available for formation of vesicles within ∼10 s.

Studies at hippocampal synapses using the pH-sensitive protein synaptopHlorin (Fernandez-Alfonso & Ryan, 2004; Li *et al.* 2005) also reported no preferential reuse of recycled vesicles. In studies using FM dyes, however, exocytosed vesicles were available, and released preferentially, after tens of seconds with low frequency stimulation (Richards *et al.* 2003; reviewed by Rizzoli & Betz, 2005). Although differences in endocytic strategies probably exist among various synapses, differing experimental protocols also may contribute to the disparity between our finding and those of others. For example, washing out FM dyes to reduce high fluorescence background requires only seconds in snake, but ∼5 min (or longer) in other preparations. This limitation complicates rapid detection of synaptic vesicle re-availability after endocytosis (Kavalali, 2006).

Future directions

One key unknown aspect of ME is its trigger, which apparently differs between snake and other preparations, notably frog. Another is the mechanism of endosome fission. Is it the same for ME from the plasma membrane and for budding of small endosomes from large ones? Our evidence is consistent with a very simple model in which ME, splitting of large endosomes into small ones and CME are all triggered as soon as activity begins, perhaps by a single mechanism. There are also many questions regarding the broader function of endosomes in nerve terminals. If vesicular proteins are selectively retrieved by CME, how are the remaining proteins in endosomes returned to the plasma membrane? How do plasma membrane proteins, vesicular membrane proteins and other molecules cease recycling to enter a degradation pathway when appropriate? A variety of experimental techniques will probably be required to answer these important questions.

References

Berthiaume EP, Medina C & Swanson JA (1995). Molecular size-fractionation during endocytosis in macrophages. *J Cell Bio* **129**, 989–998.

Conner SD & Schmid SL (2003). Regulated portals of entry into the cell. *Nature* **422**, 37–44.

de Lange RP, de Roos AD & Borst JG (2003). Two modes of vesicle recycling in the rat calyx of Held. *J Neurosci* **23**, 10164–10173.

Ertunc M, Sara Y, Chung C, Atasoy D, Virmani T & Kavalali E (2007). Fast synaptic vesicle reuse slows the rate of synaptic depression in the CA1 region of hippocampus. *J Neurosci* **27**, 341–354.

Fernandez-Alfonso T & Ryan TA (2004). The kinetics of synaptic vesicle pool depletion at CNS synaptic terminals. *Neuron* **41**, 943–953.

Gad H, Low P, Zotova E, Brodin L & Shupliakov O (1998). Dissociation between Ca^{2+}-triggered synaptic vesicle exocytosis and clathrin-mediated endocytosis at a central synapse. *Neuron* **21**, 607–616.

Heidelberger R (2001). ATP is required at an early step in compensatory endocytosis in synaptic terminals. *J Neurosci* **21**, 6457–6474.

Holt M, Cooke A, Wu MM & Lagnado L (2003). Bulk membrane retrieval in the synaptic terminal of retinal bipolar cells. *J Neurosci* **23**, 1329–1339.

Kavalali ET (2006). Synaptic vesicle reuse and its implications. *Neuroscientist* **12**, 57–66.

Koenig JH & Ikeda K (1996). Synaptic vesicles have two distinct recycling pathways. *J Cell Biol* **135**, 797–808.

Koenig JH & Ikeda K (2005). Relationship of the reserve vesicle population to synaptic depression in the tergotrochanteral and dorsal longitudinal muscles of *Drosophia*. *J Neurophysiol* **94**, 2111–2119.

Kuromi H & Kidokoro Y (1998). Two distinct pools of synaptic vesicles in single presynaptic boutons in a temperature-sensitive *Drosophila* mutant, *shibire*. *Neuron* **20**, 917–925.

Li Z, Burrone J, Tyler WJ, Hartman KN, Albeanu DF & Murthy VN (2005). Synaptic vesicle recycling studied in transgenic mice expressing synaptopHlorin. *Proc Natl Acad Sci USA* **102**, 6131–6136.

Lin MY, Teng H & Wilkinson RS (2005). Vesicles in snake motor terminals comprise one functional pool and utilize a single recycling strategy at all stimulus frequencies. *J Physiol* **568**, 413–421.

LoGiudice L & Matthews G (2006). The synaptic vesicle cycle: is kissing overrated? *Neuron* **51**, 676–677.

Miller TM & Heuser JE (1984). Endocytosis of synaptic vesicle membrane at the frog neuromuscular junction. *J Cell Biol* **98**, 685–698.

Neves G, Gomis A & Lagnado L (2001). Calcium influx selects the fast mode of endocytosis in the synaptic terminal of retinal bipolar cells. *Proc Natl Acad Sci U S A* **98**, 15282–15287.

Paillart C, Li J, Matthews G & Sterling P (2003). Endocytosis and vesicle recycling at a ribbon synapse. *J Neurosci* **23**, 4092–4099.

Pyle JL, Kavalali ET, Piedras-Renteria ES & Tsien RW (2000). Rapid reuse of readily releasable pool vesicles at hippocampal synapses. *Neuron* **28**, 221–231.

Richards DA, Guatimosim D & Betz WJ (2000). Two endocytic recycling routes selectively fill two vesicle pools in frog motor nerve terminals. *Neuron* **27**, 551–559.

Richards DA, Guatimosim C, Rizzoli SO & Betz WJ (2003). Synaptic vesicle pools at the frog neuromuscular junction. *Neuron* **39**, 529–541.

Rizzoli SO & Betz WJ (2004). The structure organization of the readily releasable pool of synaptic vesicles. *Science* **303**, 2037–2039.

Rizzoli SO & Betz WJ (2005). Synaptic vesicle pools. *Nature Rev Neurosci* **6**, 57–69.

Royle SJ & Lagnado L (2003). Endocytosis at the synaptic terminal. *J Physiol* **553**, 345–355.

Sun J-Y, Wu X-S & Wu L-G (2002). Single and multiple vesicle fusion induce different rates of endocytosis at a central synapse. *Nature* **417**, 555–559.

Takei K, Mundigl O, Daniell L & De Camilli P (1996). The synaptic vesicle cycle: a single vesicle budding step involving clathrin and dynamin. *J Cell Biol* **133**, 1237–1250.

Teng H, Cole JC, Roberts RL & Wilkinson RS (1999). Endocytic active zones: hot spots for endocytosis in vertebrate neuromuscular terminals. *J Neurosci* **19**, 4855–4866.

Teng H & Wilkinson RS (2000). Clathrin-mediated endocytosis near active zones in snake motor boutons. *J Neurosci* **20**, 7986–7993.

von Gersdorff H & Matthews G (1994). Dynamics of synaptic vesicle fusion and membrane retrieval in synaptic terminals. *Nature* **367**, 735–739.

Wilkinson RS & Lichtman JW (1985). Regular alternation of fiber types in the transverses abdominis muscle of the garter snake. *J Neurosci* **5**, 2979–2988.

Wilkinson RS & Lin MY (2004). Endocytosis and synaptic plasticity: might the tail wag the dog? *Trends Neurosci* **27**, 171–174.

Wu W, Xu J, Wu XS & Wu LG (2005). Activity-dependent acceleration of endocytosis at a central synapse. *J Neurosci* **25**, 11676–11683.

Acknowledgements

This work was supported by U.S. Public Health Service grant NS-24752.

Supplemental material

Online supplemental material for this paper can be accessed at:
http://jp.physoc.org/cgi/content/full/jphysiol.2007.130989/DC1
and
http://www.blackwell-synergy.com/doi/suppl/10.1113/jphysiol.2007.130989